Available online at www.sciencedirect.com
ScienceDirect
Polymer 48 (2007) 901–909
polymer
www.elsevier.com/locate/polymer

Modelling stiffness of polymer/clay nanocomposites

K. Hbaieb [a,*], Q.X. Wang [b], Y.H.J. Chia [a], B. Cotterell [a]

[a] *Institute of Materials Research and Engineering (IMRE), Materials Science and Characterization Laboratory, 3 Research Link, Singapore 117602, Singapore*
[b] *Institute of High Performance Computing (IHPC), 1 Science Park Road, #01-01 The Capricorn, Singapore Science Park II, Singapore 117528, Singapore*

Received 4 August 2006; received in revised form 27 November 2006; accepted 27 November 2006
Available online 8 January 2007

Abstract

Aligned nanoclay particles can be distributed randomly in a polymer matrix even at high volume fractions, but randomly oriented particles cannot be randomly distributed at high volume fractions. Instead a nanocomposite where there are clusters of nearly aligned particles is obtained. The clusters of nearly aligned particles form an effective particle with lower aspect ratio. This phenomenon which produces a nanocomposite of less stiffness than might have been expected has implications for the processing of nanoclay polymer composites.

It is shown by comparing two-dimensional to three-dimensional finite element studies that the two-dimensional model, often used because it is simpler, does not accurately predict the stiffness. The Mori–Tanaka model is shown to give a reasonably accurate prediction of the stiffness of clay nanocomposites whose volume fraction is less than about 5% for aligned particles but underestimates the stiffness at higher volume fractions. On the other hand for randomly oriented particles the Mori–Tanaka model overestimates the stiffness of clay nanocomposites.

Keywords: Finite element; Mori–Tanaka; Stiffness

1. Introduction

Polymer/clay nanocomposites are polymeric materials that are reinforced by nanoclay particles whose dimensions are in the sub-micron scale; the particles are composed of stacks of ~1 nm thick mono-layers whose in-plane dimensions range from 100 nm to 1000 nm. The thickness of the stacks depends upon how well they are intercalated or exfoliated. For enhanced functional properties of nanocomposites, full exfoliation is desired.

The Toyota group [1–3] was the first to achieve successful exfoliation of clay in nylon 6 through in situ polymerization. They have shown that inserting as little as 4.7 wt% clay into nylon 6 doubles both elastic modulus and strength. However, it is the functional properties of nanocomposites that are the main driving force in nanocomposite development. Functional properties such as barrier [4–6], flammability resistance [7] and ablation performance [8] are all greatly improved by the addition of small volume fractions of nanoclay. To find applications for this new class of materials their mechanical properties have to be sufficient to ensure mechanical reliability.

The established mechanics-based composite stiffness models, such as the Mori–Tanaka (M–T) [9–12] and the Halpin–Tsai [13–15], are only dependent on the volume fraction, aspect ratio of the particles and the elastic constants of both matrix and particles. The particle size will not affect the stiffness unless the particles affect the structure and stiffness of the adjacent polymer. Such an effect may be present if the polymer is semicrystalline, since the particles may affect the orientation of the lamellar crystallites to give a transcrystalline layer. However, even if there is a transcrystalline layer adjacent to the clay particles, Sheng et al. [16] have shown that the effect is slight.

* Corresponding author. Tel.: +65 6874 7168; fax: +65 6774 4657.
E-mail address: hb-kais@imre.a-star.edu.sg (K. Hbaieb).

0032-3861/$ - see front matter © 2006 Elsevier Ltd. All rights reserved.
doi:10.1016/j.polymer.2006.11.062

Finite element analyses of composites containing high aspect ratio plate-like particles, although accurate, are not suitable as a general method for calculating the stiffness because of their complexity. The M–T model has a good theoretical basis since it is based on the equivalent inclusion model of Eshelby [17,18] and is generally agreed to be superior to the Halpin–Tsai model particularly for composites with high aspect ratio particles [19]. However, the M–T model, though an improvement on the dilute particle concentration model of Eshelby, becomes less accurate at high particle volume fractions where there is considerable particle interaction. It is the purpose of this paper to explore the limits of the M–T model by comparing its stiffness predictions with finite element analyses.

A stiffness model does not only depend on the accuracy and robustness of the technique used, but also on the accuracy of the elastic constants. However, these constants are not known very precisely. Even in reasonably well-exfoliated clay nanocomposites the platelets can be made up of a number of intercalated silicate sheets and the spacing of the silicate sheets affects the Young's modulus and weight/volume relationship of the effective particle. The Young's modulus is a continuum parameter; when the clay exists in a single sheet, its stiffness in terms of the force–strain relation can be estimated from its structure, but the assignment of an equivalent thickness to the sheet so that the concept of stress–strain relationship can be used is not straightforward. The distribution of the aspect ratio of the clay particles is usually wide and so the appropriate aspect ratio for any model is uncertain. Moreover, the distribution of clay particles is far from uniform. The clay particles are usually not fully dispersed so that in typical epoxy/clay nanocomposites there are clusters of high particle concentration dispersed in a matrix of low particle concentration. The stiffness of clustered composite is less than that of the same volume fraction of particles that are uniformly dispersed [20]. Thus the accuracy of the modelling of the stiffness of the nanocomposite is crucially dependent on the properties of the effective particle. Since it is difficult to accurately determine the properties of the effective particle, the apparent accuracy obtained by using a finite element analysis is largely illusory. Thus it is preferable to use an analytical model, such as the M–T model, provided it is reasonably accurate.

Three-dimensional finite element models (FEMs) of nanocomposites containing plate-like particles are difficult especially if they are randomly oriented and many researchers such as Sheng et al. [16] have used plane strain two-dimensional FEMs. However, it will be shown in this paper that two-dimensional FEMs predict a Young's modulus that differs significantly from that obtained with three-dimensional FEMs and should not be used as a basis for deciding whether analytical models are sufficiently accurate to be used for nanocomposites. Gusev [21] has used a three finite element based approach to model a composite reinforced by fibers of different shape, size and distribution. A range of composite material properties, mainly those that are governed by Laplace's equation such as dielectric constant, but also including the elastic constants were modelled [21]. In the elastic example examined, the finite element results were compared with the Halpin–Tsai [13–15] model (here almost identical to the M–T predictions). For a particle volume fraction of 3%, the Halpin–Tsai considerably overestimated the stiffness for aspect ratios greater than about 20.

2. Finite element model

Both two-dimensional and three-dimensional finite element models are presented for aligned and randomly oriented clay particles which are randomly distributed. To avoid overlong computational times the representative volume element (RVE) must be reasonably small. A periodic RVE is often used, where the particles that are cut by any of the edges (or faces) of the RVE are continued from the opposite edges (or faces) with the same orientations. The parts of particles that intersect the boundary and lie outside the RVE are included in the RVE on the opposite face of the boundary. If periodic boundary conditions are used, the size of the RVE that gives acceptable scatter is minimised Gusev [22]. That is, the mean value of the elastic constants, for even RVEs containing very few particles, is close to the exact value for large composite volume. Studying a polymer composite using glass spheres, Gusev [22] found that the average C_{1111} value was less than 1.8% in error for a RVE containing only 8 spheres. The minimum number of high aspect ratio plate-like particles in a RVE to obtain a similar error is likely to be significantly higher, because the interaction volume of a plate-like particle is much larger than a spherical particle. However, in practice the implementation of periodic boundary conditions in 3D is difficult and we have used symmetric boundary which gives results very close to those obtained from periodic boundary conditions as we describe below.

The object of this paper is to assess the accuracy of the M–T model against FEM. The values chosen for the analysis are not based on any particular nanocomposite, but are representative of typical values for epoxy nanoclay composites. Thus we assume that the elastic modulus of clay is 100 times that of the elastic modulus of the polymer matrix. Since the results are given in terms of the Young's modulus of the polymer, the absolute values are not relevant. The Poisson's ratio of both particle and matrix is 0.2 and 0.35, respectively. The aspect ratio of the particles, defined as the ratio of the particle length to the particle thickness, is assumed to be 50 (or 100 for some sets of 2D calculations). In all models we assume that both the matrix and the clay particles are isotropic and are linearly elastic. The particles are assumed to be perfectly bonded to the matrix. The 2D model is subjected to plane stress.

The finite element calculations are conducted using the commercial software ABAQUS. The elements used are four node plane stress elements with reduced integration (CPS4R) for the 2D particles and matrix and 4 node 3D linear tetrahedron elements (C3D4) for the particles and matrix in 3D. The meshes are shown in Fig. 1a–d. A uniform strain is applied to one edge/face of the model as shown in Fig. 2 by applying a point force on a rigid reference node that is kinematically coupled with the ''loaded'' edge/face in the axial direction so that nodes along the loaded edge/face have to exactly follow the

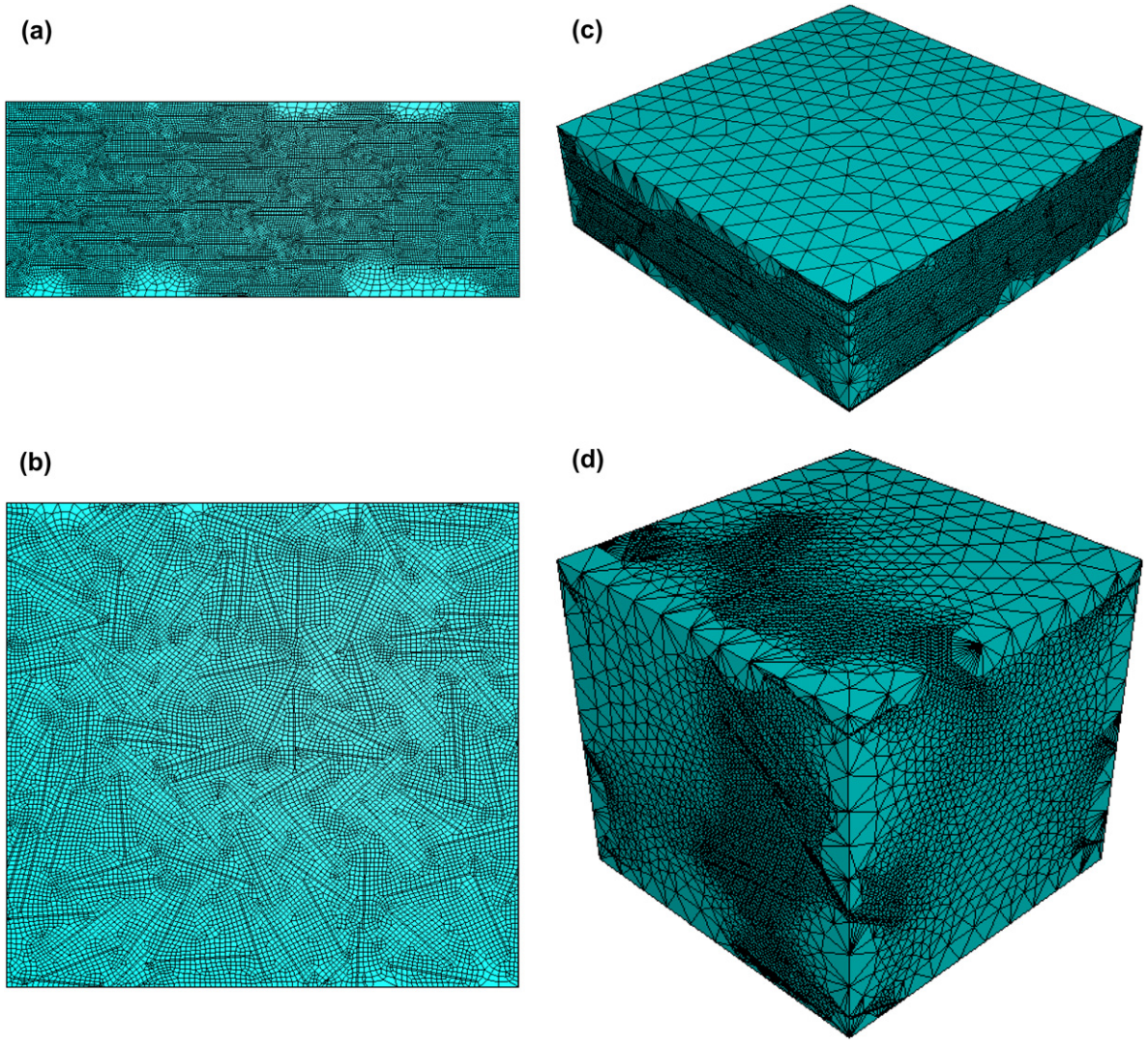

Fig. 1. Mesh details of the model for (a) 2D aligned particle distribution, (b) 2D randomly oriented-particle distribution, (c) 3D aligned particle distribution, and (d) 3D randomly oriented-particle distribution. Particle volume fraction 5%, the particle aspect ratio = 50, $E_p/E_m = 100$, $\nu_m = 0.35$, $\nu_p = 0.2$.

displacement incurred by the reference node. The stress is calculated by dividing the reaction force applied to the reference node by the area of the loaded edge/face. This procedure is better than applying a uniform displacement directly to the edge/face of the model, as the calculation of the average stress would be more cumbersome.

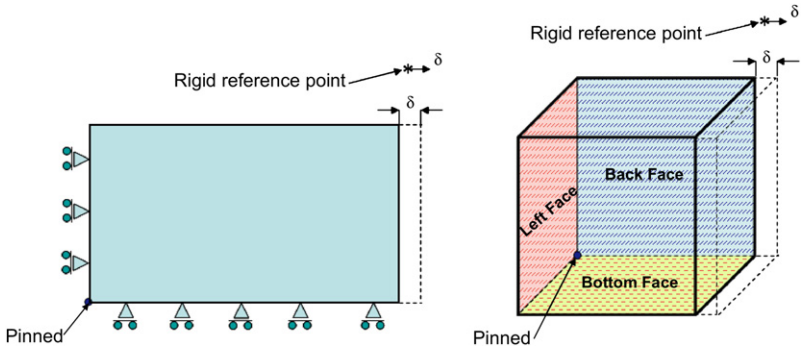

Fig. 2. Symmetric boundary conditions for both 2D and 3D FE models. For the 2D model, the bottom and left edges are lines of symmetry sharing one point that is pinned. The right edge is subjected to a uniform displacement, whereas the top edge is free of traction and any displacement constraint. For the 3D model, bottom, left and back faces are plane of symmetry. Their point of intersection is fully pinned. A uniform strain is applied to the right face, whereas the front and top faces are free of traction and displacement constraint. In either 2D or 3D model, the displacement is applied to a rigid reference node that is kinematically coupled with the right edge/face. Thus, the displacement incurred by the right edge/face is exactly the same as that applied to the rigid point.

Each calculation point is averaged over 9–10 runs corresponding to 9–10 random distributions of particles in the RVE. Individual particles, generated inside a 2D rectangle or a 3D cube, are merged with the matrix to make up the composite but yet retaining the geometrical boundaries with the matrix. The model after merging is a single entity but the elements forming the particles have different properties to those of the matrix.

2.1. Particle generation

In the 2D model the particles are 2D slender rectangles (aspect ratio 50 and 100). Fig. 3a and b shows examples of the distribution of particles in the matrix for both the aligned and random arrangement of particles. The RVE for the aligned particles is rectangular and square for the randomly oriented particles.

In the 3D model, the particle is a square plate for the aligned particles (Fig. 4a), but a disc shaped particle was used for the randomly oriented case. We modelled the particles as discs (Fig. 4b) in the randomly oriented case because the generation of non-intersecting randomly distributed particles is simpler.

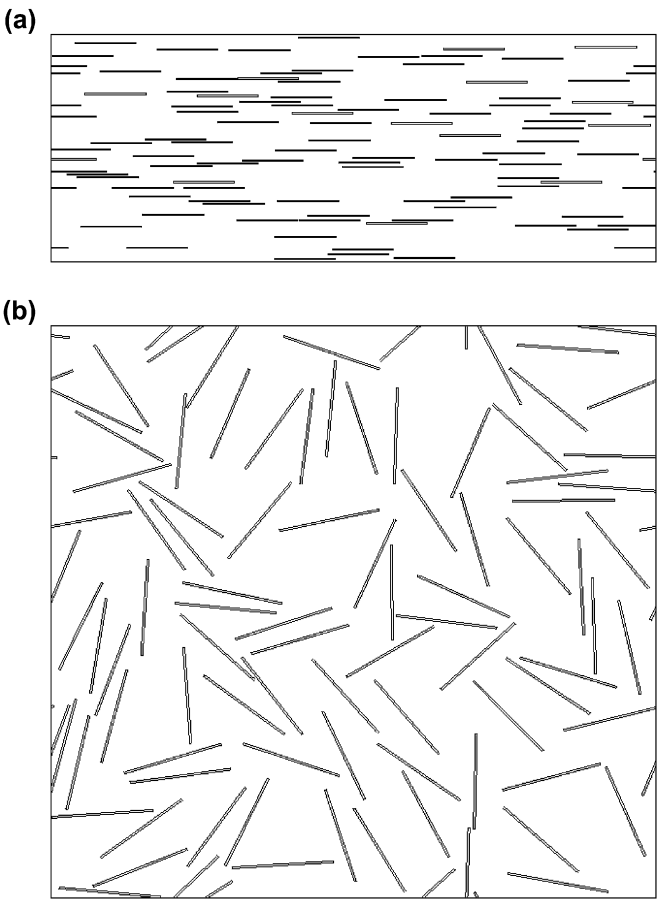

Fig. 3. (a) Two-dimensional representative volume element (RVE) including aligned particles randomly distributed. (b) Two-dimensional representative volume element (RVE) including randomly oriented particles randomly distributed. In both cases, particles that cut one of the boundaries are split into two, with the portion, that would extend beyond the boundary, moved to the opposite boundary. The volume fraction of the particles is 5%, the particle aspect ratio = 50.

For the case of the random distribution of aligned particles, a random generator is used to create the coordinates of the particle centres for both 2D and 3D configurations. A condition for non-overlapping and non-intersecting particles is enforced. The distribution of the 2D randomly oriented particles is generated by randomly creating the coordinates of a particle corner and assigning a random angle that the particle makes with the x-axis. In the 3D configuration, the centres of the discs and the components of the normal vector to the disc plane are randomly generated. In all models, a sequential generation of particles is performed. Once a particle is generated, a condition for non-overlap and non-intersection with previously generated particles is checked. If any of these conditions is violated another particle is generated and the conditions are again checked. This procedure is repeated until the whole set of particles are generated.

We have used this same arrangement for the case where symmetric (non-periodic) boundary conditions are used to ensure uniformity of particle distribution over the entire area/volume of the RVE. The size of the RVE can be very critical in obtaining accurate results; the sensitivity to the RVE dimensions is highlighted in Section 2.4.

2.2. Periodic boundary conditions

The periodic boundary conditions are applied in the 2D models for both aligned and random cases as follows:

$$\begin{aligned} u(\mathrm{RE}) &= u(\mathrm{LE}) + \delta_1, \\ v(\mathrm{RE}) &= v(\mathrm{LE}), \\ u(\mathrm{TE}) &= u(\mathrm{BE}), \\ v(\mathrm{TE}) &= v(\mathrm{BE}) + \delta_2, \end{aligned} \tag{1}$$

where RE, LE, TE, BE and δ_1 and δ_2 are the right, left, top, bottom edges and the axial and transverse displacements, respectively. The axial and transverse forces are linearly related to the applied (axial and transverse) displacements as:

$$\begin{aligned} F_x &= \alpha\delta_1 + \beta\delta_2, \\ F_y &= \gamma\delta_1 + \eta\delta_2, \end{aligned} \tag{2}$$

where $\alpha, \beta, \gamma, \eta$ are constants. The prime interest is in the elastic modulus in the axial direction, which is the direction of the particles in the aligned case, and in this case only an external force in the axial direction is applied. The transverse force should then be zero. To enforce this condition, two separate finite element calculations are carried out and the coefficient constants in Eq. (2) are determined. By setting the transverse force, in Eq. (2), to zero, the ratio of the axial to the transverse displacements can be determined. The displacements can now be applied.

There are a number of issues related to applying periodic boundary conditions with ABAQUS. One complication encountered is that the number of elements and particularly nodes has to be the same along the two opposite edges. This necessitates creating a partition at the proximity of these

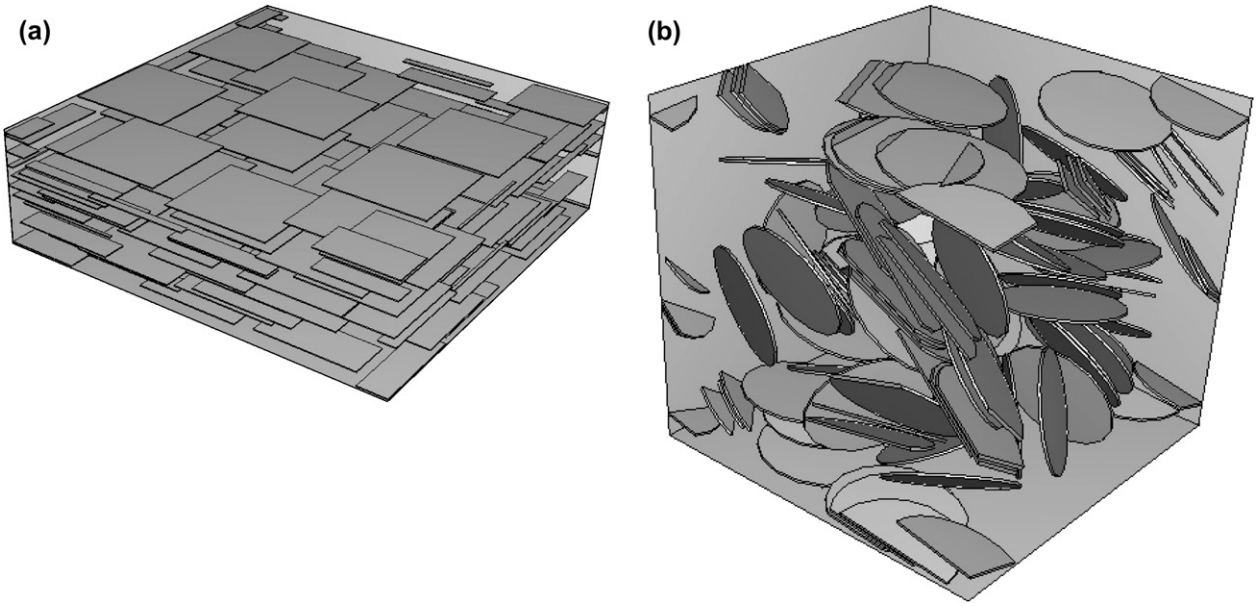

Fig. 4. (a) Three-dimensional representative volume element (RVE) including aligned clay platelets randomly distributed. The volume fraction of particles is 5%. Particles that cut one or two boundary faces are split into two or four parts with those remaining (that would otherwise be outside the RVE) relocated to opposite faces. (b) Three-dimensional representative volume element (RVE) including randomly oriented clay discs randomly distributed. The volume fraction of particles is 5%.

edges, so we can enforce the same element number and sizes to be generated along opposite edges. A further complication of applying periodic boundary conditions is that ABAQUS code orders the nodes according to the node numbers and not according to the co-ordinations. The consequence of this ordering is that the enforced kinematic constraint, whereby 2 nodes on two opposite edges will be forced to have same displacement along certain direction, will be employed on nodes having different mapping positions, that is, different relative locations along their corresponding edges. To overcome this problem, a separate simulation has to be carried out where the outputs are the node numbers and co-ordinations. The nodes are then ordered according to their locations – using a FORTRAN program – along the edges and the periodic boundary conditions are then applied at individual nodes instead of using a whole node set. In general the application of the periodic boundary condition is very involved. The techniques described above to overcome difficulties in applying periodic boundary conditions in 2D cannot be used in 3D. Similarly to the 2D case, the finite element software, ABAQUS, does not offer the option of specifying same number of nodes with one-to-one coordinate correspondence on opposite faces in 3D. The only possibility for enforcing this condition is to produce a thin partition at the vicinity of all faces, which is a very tedious process. However, even if this is accomplished the presence of particles randomly oriented in the model makes the generation of a mesh using the sweep technique impossible and instead a free mesh with tetrahedron elements must be chosen. The latter option is, however, not favourable as it is not possible to have same number of elements in two opposite faces with the nodes located in the same equivalent positions when using tetrahedron elements. Therefore, for 3D we have used symmetrical boundary conditions.

2.3. Symmetrical boundary conditions

Simple symmetrical boundary conditions are used for a RVE stressed only in an axial direction. Two edges (three faces) intersecting at a point are chosen as the lines (planes) of symmetry for the 2D case (3D case). Displacement boundary constraints are applied to these edges/faces so that no displacements occur normal to the edges/faces. Points on these edges/faces are, however, free to slide along them. In the axial direction the edge/face opposite the symmetrical edge/face is given a constant displacement in the axial direction. The other non-symmetrical edges/faces have zero stress. Except for the edges/faces which are subjected to the displacement control described above, all other edge/faces are free of any displacement constraints. Thus the boundary conditions for the 2D case with a normal strain applied in the x direction are

$$\begin{aligned} u(\mathrm{LE}) &= 0, \\ v(\mathrm{BE}) &= 0, \\ u(\mathrm{RE}) &= \delta. \end{aligned} \tag{3}$$

In addition, the top edge is free of any displacement constraint. All edges are free of shear traction and the top edge is free of normal traction as well. In the 3D case, the boundary conditions with a normal strain applied in the x direction are as follows:

$$\begin{aligned} u(\mathrm{LF}) &= 0, \\ v(\mathrm{BF}) &= 0, \\ w(\mathrm{BKF}) &= 0, \\ u(\mathrm{RF}) &= \delta, \end{aligned} \tag{4}$$

where LF, BF, BKF and RF stand for left face, bottom face, back face and right face. All other faces are free of any displacement or traction constraints.

Table 1
Differences between 2D FEM results using periodic boundary conditions with those using symmetric boundary conditions

Volume fraction	Average E_c/E_m (periodic)	Average E_c/E_m (symmetric)	Differences (%)
1%	1.3522	1.34371	0.63
3%	2.1167	2.11963	0.14
5%	3.09225	3.08009	0.39
10%	5.8497	5.722454	2.18

Both aspect ratio and ratio of particle to matrix elastic modulus, E_c/E_m, are 100. Poisson's ratios of the particle and matrix materials are 0.2 and 0.35, respectively.

We have carried out 2D finite element calculations for aligned particles using both periodic and symmetrical boundary conditions. Displacement is applied to the right edge and the resultant average stress is inferred. The particle aspect ratio is taken to be 100 and the ratio of the particle elastic modulus to the matrix elastic modulus is set at $(E_p/E_m) = 100$. The volume fraction of the particles is varied from 1% to 10%. The differences in the elastic constant calculated from finite elements using periodic and symmetric boundary conditions are given as a function of volume fraction in Table 1. Good agreement is shown between both sets of finite element results. This result implies that using symmetric boundary conditions has very little effect on the accuracy of the results and hence there is no point of using the more complicated periodic boundary conditions.

2.4. RVE size sensitivity

We have carried out several calculations for the aligned particles both in 2D and 3D configurations using 10, 30 and 100 particles for a volume fraction of 1% using symmetrical boundary conditions. These results are given in Table 2. For both 2D and 3D simulations, the results are insensitive to the RVE size provided more than 30 particles are within the RVE. Again this result proves the validity of using symmetric boundary conditions. In the subsequent analysis we have employed RVEs that contain 50–100 particles and have used symmetric boundary conditions.

3. Mori–Tanaka model

The M–T model, based on the equivalent inclusion of Eshelby [17], models the clay particle as an oblate spheroid, whereas in the finite element model we have assumed that the particles have constant thickness. Steif and Hoysan [23] have defined an elastic reinforcement factor by:

Table 2
Effect of the number of particles in the representative volume element on the finite element results

Number of particles	2D FEM results	Standard deviation (2D)	3D FEM results	Standard deviation (3D)
10	1.216338	0.009794	1.255076	0.030341
30	1.20392	0.009213	1.27623	0.013438
100	1.210608	0.004213	1.271925	0.00721

$$E_p/E_m = 1 + \lambda v_p, \tag{5}$$

where E_p is the particle elastic modulus, E_m is the matrix elastic modulus and v_p is the particle Poisson's ratio. They compared the elastic reinforcement factor, λ of cylinders and ellipsoids albeit for a low aspect ratio of 4. They showed that the aspect ratio of an ellipsoid, which had the same reinforcement factor as a rod, was less than the ellipsoid inscribed within the rod but greater than the ellipsoid that had the same length and volume as the rod. Since the rod diameter is greater than the average diameter of the inscribed ellipsoid, but is smaller than the ellipsoid of the same length and volume, shear lag theory qualitatively supports this result. However, the advantage of the M–T model, as a simple model to apply, is lost if attempts are made to improve on it empirically. Here the expressions given by Tandon and Weng [11] for the M–T model have been used to calculate the elastic modulus for aligned particles and the expressions of Wang and Pryz [12] for the randomly oriented particles.

4. Results

4.1. Aligned particles

Finite element simulations are carried out for the aligned particles for 2D and 3D configurations. Figs. 5 and 6 show the finite element results of the composite elastic modulus, E_c, normalized by the matrix elastic modulus, E_m, as a function of the volume fraction of clay particles and the predictions of the M–T model for particle aspect ratios of 100 and 50, respectively. As shown in Fig. 6, the 2D FEM results are consistently lower than those for 3D, hence testing the accuracy of the M–T model should not be made on the basis of 2D models as has frequently been the case. As shown for the case of particle aspect ratio of 50, the M–T model is very close to the 3D FEM results for volume fractions of less than 5%. For higher volume fraction, however, the M–T model significantly underestimates the 3D FEM results. The difference between

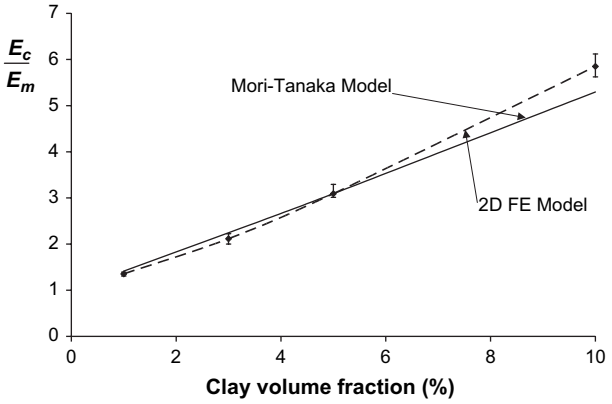

Fig. 5. Results of the ratio of the composite elastic modulus E_c to the matrix elastic modulus E_m versus filler volume fraction. Both Mori–Tanaka and 2D FEM results, for aligned particles randomly distributed, are illustrated for comparison. Particle aspect ratio AR = 100, $E_p/E_m = 100$, $v_m = 0.35$, $v_p = 0.2$.

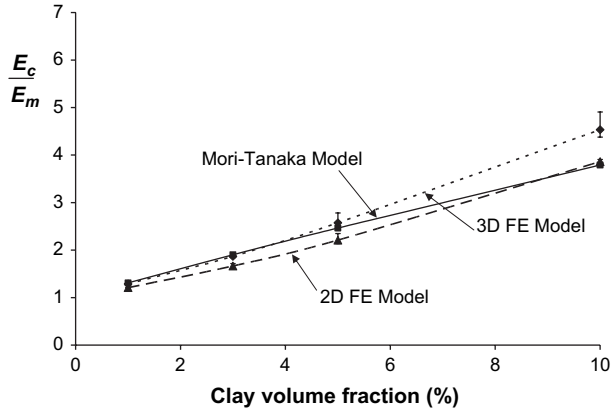

Fig. 6. Comparison of Mori–Tanaka, 2D and 3D FEM results of the composite to matrix elastic modulus ratio E_c/E_m versus clay volume fraction for aligned particles randomly distributed. Aspect ratio AR = 50, $E_p/E_m = 100$, $v_m = 0.35$, $v_p = 0.2$.

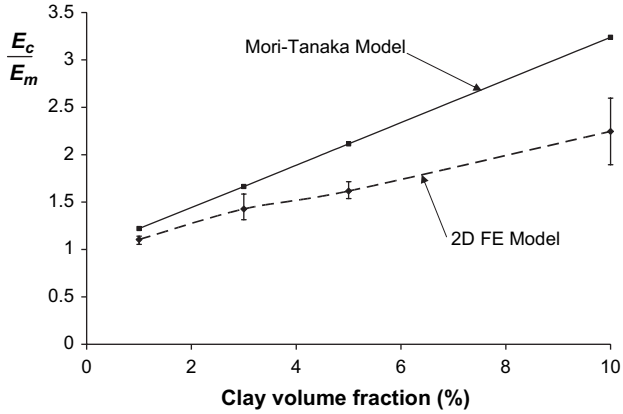

Fig. 7. Comparison of Mori–Tanaka, 2D finite element results of the composite elastic modulus normalized by the matrix elastic modulus, E_c/E_m, as a function of clay volume fraction for particles randomly distributed in all direction. The calculations are performed for particle to matrix elastic modulus ratio of 100. The particle aspect ratio is 100. The particle and matrix Poisson's ratios are 0.2 and 0.35, respectively.

the finite element results and the M–T model as function of volume fraction are given in Table 3.

4.2. Random particles

The composite elastic modulus, E_c, normalized by the matrix elastic modulus, E_m, as a function of the volume fraction of clay particles of both the finite element and the M–T model for the randomly oriented particles is shown in Fig. 7 for particle aspect ratio of 100 and in Fig. 8 for particle aspect ratio of 50. The elastic modulus obtained from the 2D finite element simulation again significantly underestimates the elastic modulus obtained from the 3D simulation (Fig. 8). There were difficulties in performing 3D FEM simulations for volume fraction of 10%. The problem is that, with a random orientation, it is impossible to generate particles that do not intersect. In practice it means that a fully exfoliated and randomly oriented polymer/clay composite cannot be processed for volume fractions greater than about 5% which agrees with experiment. Therefore the 3D finite element results could not be obtained for greater than 5% volume fraction. The M–T model overestimates the elastic modulus and the difference between it and finite element simulation is given in Table 3.

5. Discussion

A 3D configuration should be used to model any property of a composite. However, some researchers have used 2D models to approximate the behaviour of composites. We have shown by performing both 2D and 3D FEMs that the 2D FEM cannot be used to accurately predict the stiffness of a nanoclay polymer composite. As we have demonstrated that 2D results are consistently lower than 3D results, we believe that the better agreement of 2D FEM results with experimental results as compared to M–T prediction, reported by Sheng et al. [16], is due to the artefact that using 2D model will necessarily give lower values of elastic modulus. In our analysis we have compared 3D FEM with the M–T model for both aligned and random cases. In the aligned case, we have shown that at high clay volume fraction, the 3D FEM results are progressively larger than the M–T predictions. It is believed that this underestimate by the M–T model is due to the interaction between clay particles, caused by their high aspect ratio. The interaction between particles, which becomes more important for the higher clay contents, is not modelled by M–T model, which is most accurate for dilute systems. Sheng et al. [16] have very well explained the consequences of two particles approaching each other. If two particles are at approximately the same height and are close to each other in the axial direction, they interact with each other such that they form an equivalent effective particle with higher aspect ratio that will contribute to higher stiffening.

With randomly oriented particles the M–T model results clearly overestimate the elastic modulus and the difference

Table 3
Comparison between M–T predictions and 2D and 3D finite element results for both aligned and random cases

Volume fraction	Mori–Tanaka aligned	2D FEM aligned	3D FEM aligned	Mori–Tanaka random	2D FEM random	3D FEM random
1%	1.31	1.2106075	1.288233	1.14	1.068075	1.150495
3%	1.901	1.66514	1.86094	1.43	1.22595	1.3469
5%	2.463444	2.20872	2.575	1.73	1.3837	1.55955
10%	3.79	3.86137	4.535	2.5	1.6595	

The particle aspect ratio is 50. The ratio of particle to matrix elastic modulus is 100. The Poisson's ratios of particle and matrix materials are 0.2 and 0.35, respectively.

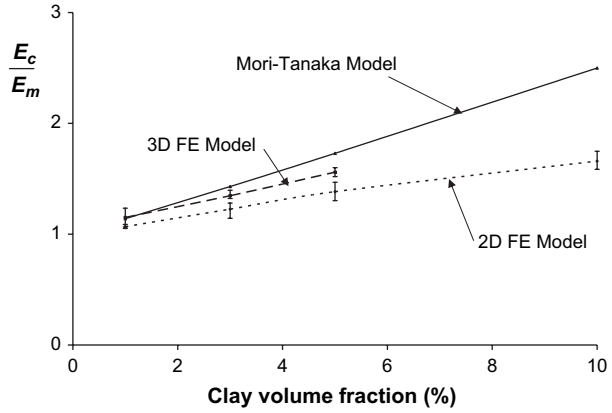

Fig. 8. Comparison of Mori–Tanaka, 2D and 3D finite element results of the composite elastic modulus normalized by the matrix elastic modulus, E_c/E_m, as a function of clay volume fraction for particles randomly distributed in all direction. For clay volume fraction higher than 1%, the Mori–Tanaka results are clearly higher than finite element results. The calculations are performed for particle to matrix elastic modulus ratio of 100. The particle aspect ratio is 50. The particle and matrix Poisson's ratios are 0.2 and 0.35, respectively.

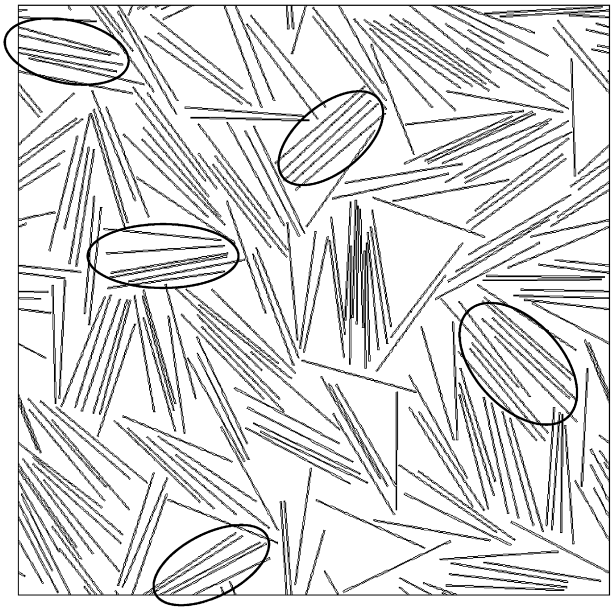

Fig. 9. Particle distribution for the random 2D FE model at particle volume fraction of 10%. A few circles are drawn to highlight examples of parallel stacking of particles. These stacks form effective particles of small aspect ratio which decrease the capability of the composite stiffening by the introduction of clay particles of very high stiffness.

increases with increasing volume fraction. It might be expected that the interaction that has led to the M–T model underestimating the stiffness for the aligned case would do the same for the randomly oriented case. Our results show that this is not the case. The M–T model assumes that the volume fraction is small so that there is no interaction between particles. However, with randomly oriented particles there is not only strong interaction between particles at the higher volume fractions, but also the randomness of the orientation is affected. At higher volume fractions the particles tend to stack together on top of each other to form clusters where the particle orientation is similar. These clusters form effective particles of lower aspect ratios. In the 2D configuration, particles have to rearrange on one plane and clustering of parallel particles is more likely, as is clearly shown in Fig. 9. This particle clustering is particularly noticeable at high volume fractions and causes a decrease in stiffness. Thus, the interaction between particles that caused an increase in stiffness as compared with M–T model for the aligned case has now caused a decrease in stiffness. This phenomenon is not limited to the model, but also will affect the elastic modulus of real polymer/clay nanocomposites. If attempts to produce a fully exfoliated nanocomposite with random orientation succeed at high volume fraction then clusters of particles of similar orientation will form and the elastic modulus will be less than that might have been expected.

In summary, the 2D FEM results are consistently lower than the 3D FEM results for both aligned and randomly oriented particles. This difference in behaviour is because, in 3D there is stiffening in the both axial and transverse directions, whereas in 2D stiffening can only occur in the axial direction. The stiffening in the transverse direction induces a lower Poisson's ratio due to the lower transverse strain which contributes to the increase of the overall stiffening of the composite. The comparison of the M–T prediction with 3D FEM results has revealed two different phenomena depending on whether the particles are aligned or randomly distributed. In the aligned case, M–T model gives a very good prediction of the elastic modulus for the practical range of clay volume fractions (1–5%). At larger volume fractions, M–T model underestimates the elastic modulus, since it does not account for the interaction between particles. The 3D FEM, however, does model the interaction between particles and therefore predicts a higher composite elastic modulus. The increase of the stiffening effect is due to the formation of some effective particles with higher aspect ratios. The random generation of the aligned particles may cause one particle to be in very close proximity to another particle. The region of the matrix enclosed between the particles is highly constrained so that it behaves as if it were almost an integral part of the two particles. The consequence is that an effective particle is formed with higher aspect ratio and therefore a further increase in stiffness. This observation suggests that M–T model is limited to low volume fraction up to 5%.

For the case of randomly oriented particles, however, the random distribution causes formation of clusters of nearly parallel particles. The condition that particles do not intersect, combined with the fact that the particles can be oriented in any direction, causes some of the matrix to be free of any particles. As the matrix between a stack of nearly parallel particles is highly constrained, the whole cluster of particles forms an effective particle with much lower aspect ratio. This kind of interaction is not considered in the M–T model and hence there is limitation to the M–T model when considering distribution of randomly oriented particles. It is due to this real phenomenon that the M–T model consistently overestimates the 3D FEM results.

6. Conclusions

Two-dimensional models do not predict the elastic modulus of real polymer/clay nanocomposites accurately.

If the particles are aligned the M–T model will accurately predict the elastic modulus up to volume fractions of about 5% but will underestimate the elastic modulus at higher volume fractions.

Fully exfoliated randomly oriented polymer/clay nanocomposites cannot be processed at high volume fractions but clusters of particles with nearly the same alignment form. The elastic modulus of such nanocomposites is less than that might at first be expected and here the elastic modulus is overestimated by the M–T model.

References

[1] Usuki A, Kojima Y, Kawasumi M, Okada A, Fukushima Y, Kurauchi T, et al. Journal of Materials Research 1993;8:1179.
[2] Kojima Y, Usuki A, Kawasumi M, Okada A, Fukushima Y, Kurauchi T, et al. Journal of Materials Research 1993;8:1185.
[3] Kojima Y, Usuki A, Kawasumi M, Okada A, Kurauchi T, Kamigaito O. Journal of Applied Polymer Science 1993;49:1259.
[4] Yano K, Usuki A, Okada A, Kurauchi T, Kamigaito O. Journal of Polymer Science Part A: Polymer Chemistry 1993;31:2493.
[5] Messersmith PB, Giannelis EP. Chemistry of Materials 1994;6:1719.
[6] Messersmith PB, Giannelis EP. Journal of Polymer Science Part A: Polymer Chemistry 1995;33:1047.
[7] Gilman JW. Applied Clay Science 1999;15:31.
[8] Vaia RA, Price G, Ruth PN, Nguyen HT, Lichtenhan J. Applied Clay Science 1999;15:67.
[9] Mori T, Tanaka K. Acta Metallurgica 1973;21:571.
[10] Benveniste Y. Mechanics of Materials 1987;6:147.
[11] Tandon GP, Weng GJ. Polymer Composites 1984;5:327.
[12] Wang J, Pryz R. Composites Science and Technology 2004;64:925.
[13] Ashton JE, Halpin JC, Petit PH. Primer on composite materials: analysis. Stamford Conn: Technomic; 1969.
[14] Halpin JC. Journal of Composite Materials 1969;3:732.
[15] Halpin JC, Kardos JL. Polymer Engineering and Science 1976;16:344.
[16] Sheng N, Boyce MC, Parks DM, Rutledge GC, Abes JI, Cohen RE. Polymer 2004;45:487.
[17] Eshelby JD. Proceedings of the Royal Society of London Series A 1957;241:376.
[18] Eshelby JD. Elastic inclusions and inhomogeneities. In: Sneddon IN, Hill R, editors. Progress in solid mechanics, vol. 2. Amsterdam: North Holland; 1961. p. 89–140.
[19] Tucker C, Liang E. Composite Science and Technology 1999;59:671.
[20] Luo JJ, Daniel M. Composites Science and Technology 2003;63:1607.
[21] Gusev AA. Macromolecules 2001;34:3081.
[22] Gusev AA. Journal of the Mechanics and Physics of Solids 1997;45:1449.
[23] Steif PS, Hoysan SF. Mechanics of Materials 1987;6:197.